AJNR Am J Neuroradiol 21:1055–1063, June/July 2000

The Influence of Gliomas and Nonglial Space-occupying Lesions on Blood-oxygen-level–dependent Contrast Enhancement

Axel Schreiber, Ulrich Hubbe, Sargon Ziyeh, and Jürgen Hennig

BACKGROUND AND PURPOSE: **Functional MR (fMR) imaging with blood-oxygen-level–dependent (BOLD) contrast enhancement is increasingly used as a noninvasive tool for presurgical mapping in patients with intracranial tumors. Most physiologic studies of task-related BOLD contrast enhancement have involved healthy volunteers. Therefore, it is not known whether BOLD contrast is evoked in the same way in or adjacent to tumor tissue. The purpose of this study was to study the influence of different intracranial tumors on BOLD contrast enhancement.**

METHODS: **fMR mapping of the sensorimotor cortex was successfully performed in 15 of 21 patients with intracranial space-occupying lesions by using a bimanual motor task. Tumors were located either within the sensorimotor area itself or in adjacent brain areas, inducing changes of signal intensity on T2-weighted images along the pre- or postcentral gyrus. Space-occupying lesions were divided into a group comprising gliomas (seven cases) and a group comprising nonglial space-occupying lesions (three metastases, two cavernomas, one abscess, one arteriovenous malformation, one meningioma). A hemispheric activation index was calculated using the volume of activation on the affected and on the contralateral hemisphere. Hemispheric activation indices of gliomas and nonglial lesions were compared statistically.**

RESULTS: **The activated volume in the hemispheres ipsilateral to the nonglial lesions was 14% larger than in the contralateral hemisphere, whereas in the hemispheres ipsilateral to gliomas, the activated volume decreased by 36% in comparison with the contralateral hemisphere. The difference between nonglial lesions and gliomas was significant ($P < .05$).**

CONCLUSION: **The generation of BOLD contrast enhancement is reduced near gliomas but is not affected by nonglial tumors.**

Functional MR (fMR) imaging using blood-oxygen-level–dependent (BOLD) contrast enhancement is increasingly being used as a noninvasive tool for the presurgical mapping of cortical function in patients with intracranial tumors (1–5). Until now, most physiologic studies of task-related BOLD contrast enhancement have been limited to healthy volunteers. It is not known whether BOLD contrast enhancement is evoked in the same way in or adjacent to tumor tissue. The evolution of BOLD contrast enhancement depends on structural properties of the brain, such as the cortical blood volume, density, size, and topography of cortical vessels; physical properties, such as water diffusion coefficient (6–9); and the ultrastructural composition of the cortex, such as the cellular contacts between capillaries and astrocytes and neurons (10). In addition, metabolic properties of the brain, such as the oxygen extraction fraction in the cortex, glucose metabolism, and neurotransmitter distribution, particularly of those involved in neurovascular coupling (11), may also affect BOLD contrast enhancement.

Intracranial space-occupying lesions alter some or all of these properties. They induce proliferation of pathologic vessels in the adjacent tissue, thus altering density, size, and topography of vessels and increasing the blood volume (12–14). The blood-brain barrier is broken down within the tumor mass and partially breached in the tissue adjacent to the tumor (15). The resulting vasogenic edema has been shown to change the apparent dif-

Received August 5, 1999; accepted after revision January 7, 2000.

From the Departments of Neurology (A.S.), Neurosurgery (U.H.), Neuroradiology (S.Z.), and Radiology (J.H.), Albert-Ludwigs-University, Freiburg, Germany.

Presented in part at the 5th Scientific Meeting of the International Society for Magnetic Resonance in Medicine, Vancouver, 1997, and the 5th International Conference on Functional Mapping of the Human Brain, Dusseldorf, 1999.

Address reprint requests to Axel Schreiber, MD, Woehlerstraße 26, 67133 Maxdorf, Germany.

fusion coefficient (16). Positron emission tomographic studies of patients with gliomas have shown decreases in oxygen extraction within the tumor and global increases in the cortex. In the same patients, cerebral blood flow to the cortex is globally decreased (17–19). Within the zone of gliomatous invasion, the cortex ultrastructure is altered. Preexisting blood vessels are deprived of their glial sheaths as reactive astrocytes retract their end feet (20). Although neurons show little destructive change during the early stages of invasion, even when surrounded by neoplastic cells, their cellular contacts with the astrocytes and the capillary bed are reduced. The biochemical environment (adenosine 5′-triphosphate, pH, glucose, lactate, etc. [21, 22]) and the cortical levels of neurotransmitters in and around gliomas are altered. Specifically, the release of nitric oxide by reactive astrocytes and macrophages at the brain-glioma interface may increase the regional cerebral blood flow (23).

In this study, we compared the effects of glial and nonglial space-occupying lesions on BOLD contrast enhancement in the sensorimotor area. We predicted that glial tumors would affect BOLD contrast enhancement more than nonglial tumors because of their structural and functional differences. Neuroepithelial tumors, such as gliomas, diffusely infiltrate adjacent brain parenchyma (12, 24). In contrast, other space-occupying lesions are delineated from normal tissue, at least at the microscopic level. Neuroglial tumors, therefore, alter the cellular architecture of the brain, whereas nonglial lesions may cause macroscopic deformation without substantially affecting cellular architecture in the perilesional area. In addition to structural changes, gliomas have the capacity to elaborate neurotransmitters as they are derived from glial cells that play an important role in releasing and eliminating transmitter substances from the synaptic cleft (25). We would thus expect glial tumors to have an effect on cortical metabolism and neurovascular coupling. The purpose of this study was to compare the effect of gliomas and nonglial space-occupying lesions on BOLD contrast enhancement.

Methods

We used a simple bimanual motor task to elicit BOLD contrast enhancement in the sensorimotor cortex of both hemispheres in 21 patients. In the 15 patients with successful results of their fMR imaging examinations, the volume of activation on the hemisphere ipsilateral to the space-occupying lesion was normalized to the volume of activation on the hemisphere contralateral to the space-occupying lesion (referred to as the contralateral or ipsilateral hemisphere, respectively) by calculating a hemispheric activation index (HAI). Parameters of the tumors that we suspected to have influence on BOLD contrast enhancement were tumor volume, distance of the tumor to the hand-motor area and its displacement by the tumor, age of the patient, and type of tumor (glioma versus nonglial lesion). Stepwise multiple regression was used to determine the parameters that best accounted for the variability of the HAI.

Patient Selection

For a period of 18 months, we included patients suffering from intracranial space-occupying lesions in the study. The lesions were located within the pre- or postcentral gyrus or at least altered the MR signal within the pre- or postcentral gyrus when located elsewhere in the frontal or parietal brain. In addition to the neurologic status assessed by the department of neurosurgery, the motor system was examined before fMR imaging was performed. The symptoms were classified into three categories: 1) without signs of pathologic abnormalities (normal muscle strength and tone in comparison with the contralateral side), 2) mild motor deficits (muscle strength reduced in comparison with the contralateral side but repeated motion against gravitational force possible without fatigue) (Table), and 3) major motor deficits (motion against gravitational force reduced). Patients with major motor deficits of the upper extremities, patients with contraindications to MR imaging, or patients who were not cooperative for other reasons were excluded. The participants were informed regarding the experimental procedure, and the paradigm was trained. All participants provided informed consent to participate in the study. A total of 21 patients were studied; 15 cases were successful. Of the successful cases, seven patients suffered from gliomas (five astrocytomas, one glioblastoma multiforme, one ependymoma) and eight patients suffered from intracranial space-occupying lesions of nonglial origin (three metastases, three vascular malformations, one meningioma, one abscess) (Table). At the time of the fMR imaging examination, 19 patients were treated with antiepileptic drugs (14 patients presented with epileptic seizures initially) and 15 with steroids. Among the patients in the group with gliomas (nonglial lesions) who had successful results of their fMR imaging, seven (6) were treated with antiepileptic drugs and seven (4) with steroids; three (5) presented with epileptic seizures. Handedness was assessed using the Edinburgh handedness inventory (26). The tumor diagnosis was confirmed histologically.

MR Imaging

Participants were positioned in a 1.5-T Siemens Magnetom Vision imager (Siemens, Erlangen, Germany) equipped with a vacuum cast (Tellewa AG, Adlikon, Switzerland) to reduce head motion. Earphones were put on to shield the ears against the gradient noise and to maintain the communication with the operator. For functional imaging, we used a blipped, multisection echo-planar sequence (3500/84 [TR/TE]; flip angle, 90°), with a matrix of 128 × 128 pixels and a field of view of 256 × 256 mm^2. Parallel to a line connecting the genu with the splenium corporis callosi (structures visible on the sagittal scout image), 8 to 12 axial sections with 4-mm thickness were acquired covering the sensorimotor cortex of the upper limb. The spatial resolution was 2 × 2 × 4 mm^3. Before the fMR imaging was performed, an automated shimming procedure was used to optimize B_0 homogeneity. Each section was imaged 64 times during 224 s. The first two images were discarded to allow for steady-state saturation of tissue magnetization. The motor task was arranged in a block design, alternating 28 s of rest with 28 s of bimanual opening and closing of the hands at approximately 1 Hz. The operator informed the participants by earphones when to start and when to stop the hand movement. The motion of the hands was monitored regarding frequency, extent, and bimanual symmetry.

Anatomic sections were acquired in the same position as the functional images, using a T2-weighted turbo spin-echo sequence (4500/120; flip angle, 180°), with an in-plane resolution of 0.61 × 0.45 mm^2. Whole-brain anatomic images were acquired as a 3D T1-weighted, magnetization-prepared–rapid-acquisition–gradient-echo (MPRAGE) sequence (9,7/4; flip angle, 12°), covering the entire head (175 mm ear to ear

Results and characterization of space-occupying lesions in patients who underwent successful FMR imaging

Case (No.)	Pathologic Diagnosis, Location	Presenting Symptoms	A_i/A_c (voxels)	HAI	Volume (cm^3)	Distance (mm)	Displacement (mm)	Enhancement	Age (yrs)/Sex	Handedness
3	Metast. (carcinoma), l. prec. g.	Mild aphasia	234/225	1.08	1.7	22	8	Y	49/F	R/D
4	Abscess, l. prec. g.	Mid paresis (r. hand), seizures	181/168	1.08	0.13	0	7	Y	52/F	R/D
5	Cavernoma, r. prec. g.	Seizures	226/153	1.48	3.2	10	0	N	47/M	R/N
6	Metast. (lung cancer), l. frontal	Seizures	53/225	0.24	4.1	8	2	Y	64/M	R/D
7	Cavernoma, l. postc. g.	Seizures	188/118	1.59	2.0	5	6	N	33/F	R/D
8	Arteriovenous angioma, l. frontal	Seizures	84/114	0.74	4.2	20	6	Y	44/F	R/D
9	Meningioma, r. parietal	Hypaesthesia l. arm	149/114	1.31	0.7	17	4	Y	58/F	R/N
10	Metast. (lung cancer), r. postc. g.	Hemiparesis l.	103/63	1.63	9.6	5	17	Y	68/M	R/N
Average values of nonglial space-occupying lesions		—	153/148	1.14	3.0	11	6	—	52	—
12	Astrocytoma, WHO III, l. frontal	Seizures	115/238	0.48	6.9	10	0	Y	57/F	L/N
13	Ependymoma, WHO III, l. parietal	Hemianopsia r.	52/80	0.65	220.0	10	26	Y	27/F	R/D
14	Glioblastoma, WHO IV, l. prec. g.	Mild paresis, r. hand	37/106	0.35	4.4	0	7	Y	76/F	R/D
15	Astrocytoma, WHO III, l. frontal	Headache	77/70	1.10	61.0	46	8	Y	61/M	R/D
16	Astrocytoma, WHO II, r. parietal	Seizures	73/64	1.14	25.0	9	8	N	29/F	R/N
17	Astrocytoma, WHO III, r. parietal	Mild hemiparesis l.	47/151	0.46	170.0	10	23	Y	36/M	R/N
20	Astrocytoma, WHO III, r. prec. face	Seizures l., face	215/470	0.31	72.0	10	7	N	22/F	R/N
Average values of gliomas		—	88/168	0.64	80.0	14	11	—	44	—

Note.—A_i = volume of activation on the ipsilateral hemisphere; A_c = volume of activation on the contralateral hemisphere; metast. = metastasis; l. = left; prec. g. = precentral gyrus; R = right handed; D = tumor on dominant hemisphere; r. = right; N = tumor on non-dominant hemisphere; postc. g. = postcentral gyrus; L = left handed.

times 256 × 256 mm^2), with an isotropic spatial resolution of 1 mm^3.

Image Processing

All fMR imaging experiments were corrected for head motion by using a voxel-based cross-correlation algorithm referenced to the first set of images. This first set of images was coregistered with the 3D image of the brain by using a local elastic-matching algorithm based on Beziér splines. The spline-defining grid had a mesh size of 16 mm^3, leading to a total number of approximately 150 control points within the measured volume. Each control point could be relocated in three dimensions under elastic constraint (27). Statistical significance of changes in signal intensity was calculated on a voxel-by-voxel basis using Student's *t* test. To account for hemodynamic latencies, the rest/activity pattern was shifted by one data point (3.5 s). Voxels with *P* less than .025 were displayed in the activation map. The activation map was spatially filtered using a median filter (3 × 3 matrix). The probability of false-positive voxels occurring randomly was reduced by this procedure to 2×10^{-6}. The signal time courses of the remaining clusters of activated voxels were examined. Clusters showing more than 9% increase of signal from the rest to the activation condition were suspected to be due to flow or head motion and were therefore excluded from further analysis. Clusters showing no adequate hemodynamic delay (at least 3.5 s or one image) were suspected to result from head motion and were excluded as well. The volume of the clusters of activation in the sensorimotor cortex (in most cases only one cluster per hemisphere) that were qualified by their signal time course was calculated for the contralateral (A_c) and for the ipsilateral (A_i) hemisphere.

On the 3D images, the maximum extent of the space-occupying lesions was measured in three orthogonal directions (*x, y, z*) and the volume of the space-occupying lesions was estimated as an ellipsoid with the volume: $V = \pi \times x \times y \times z/6$. The localization of the hand-motor area was determined on the 3D image as the Ω-shaped formation of the precentral gyrus (28, 29), if this was possible to do without doubt. In the remaining cases, the hand-motor area, as determined by fMR imaging, was used as a clue regarding where to look for the hand-motor area in the 3D image. In these cases, the typical, although distorted, form of the hand-motor area could be recognized ex post facto. The distance between the space-occupying lesion and the hand-motor area was measured. The displacement of the hand-motor area, attributable to the space-occupying lesion, was estimated as the distance between the actual hand-motor area on the ipsilateral hemisphere and the hand-motor area of the contralateral hemisphere mirrored at the median sagittal plane, assuming lateral symmetry of the central sulcus (30, 31).

Statistical Evaluation

Because of the large interindividual variance of the volume of activation (32, 33), the activated volume on the ipsilateral hemisphere was normalized to the activated volume on the contralateral hemisphere by calculating the HAI as $HAI = A_i/A_c$. HAIs were statistically compared with a balanced activation, with HAI = 1 as expected in healthy participants (hemispheric symmetry in activation). Using SPSS (SPSS Inc., Chicago, IL), stepwise multiple regression was performed to test which of the parameters (volume of the space-occupying lesion, distance to the hand-motor area, displacement of the hand-motor area, or type of tumor [glioma versus nonglial lesion]) best predicted the HAI. The *P* value was set to less than .05 to enter a parameter in forward model selection and to greater than .05 to remove a parameter in backward model selection. The effects of paresis of the hand contralateral to the tumor, tumor on the dominant versus nondominant hemisphere, and type of tumor on the HAI were studied using analysis of variance.

Results

fMR imaging was considered successful if the sensorimotor cortex on the contralateral hemisphere could be localized because of the BOLD contrast enhancement or if the participants had cooperated during the measurement and the fMR imaging data were free from artifact, even if there was no BOLD contrast enhancement. For 15 (71%) of the 21 patients examined, fMR imaging was successful and the sensorimotor cortex could be localized on the contralateral as well as on the ipsilateral hemisphere. Because of head motion that could not be corrected, six (29%) functional data sets had to be discarded. Three of these were from patients who had neuropsychological deficits and were not fully able to keep still. All artifact-free examinations showed BOLD contrast enhancement on the ipsilateral or the contralateral hemisphere. The mean HAI of all 15 successful experiments was 0.91, with an SD of 0.48 (Table). In these patients, the distribution of frequencies of the hand motion was bimodal, with one peak with the imager pace at 1.14 Hz and a second peak at 0.95 Hz. The mean frequency was 1.03 Hz, with an SD of 0.1 Hz. The frequencies did not correlate significantly with the total volume of activation or with the HAI. The frequency and phase of the hand motion was bimanually symmetrical in all patients.

Adjacent to nonglial tumors, a normal volume of BOLD contrast enhancement was elicited. Neither the proximity of the space-occupying lesion (Fig 1A) nor white matter edema directly extending into the pre- and postcentral gyrus nor the displacement of the sensorimotor cortex of the hand (Fig 1B) influenced the activated volume. On average, the activated volume in the ipsilateral hemisphere was 14% larger than in the contralateral hemisphere, although this deviation from a balanced distribution (HAI = 1) did not prove to be significant (mean HAI, 1.14; SD, 0.47).

BOLD contrast enhancement was reduced near gliomas, as indicated by the mean HAI of 0.64 (SD, 0.34) in this group of patients. The distribution of HAIs significantly differed between the patients with nonglial lesions and the patients with gliomas (*t* test, $P < .01$). The mean HAI in the glioma group differed significantly ($P < .01$) from 1 (balanced distribution) also. In two patients (cases 14 and 20) with gliomas, the hand-motor cortex showed T2 signal hyperintensity, suggesting gliomatous infiltration (34, 35). No BOLD contrast enhancement was evoked on the infiltrated cortex (Fig 2) in either case, although there was BOLD contrast enhancement on the adjacent cortex showing no T2 signal hyperintensity.

Only the type of tumor (glioma or nonglial lesion) significantly ($P < .05$) correlated with the HAI. The other parameters (volume of the space-

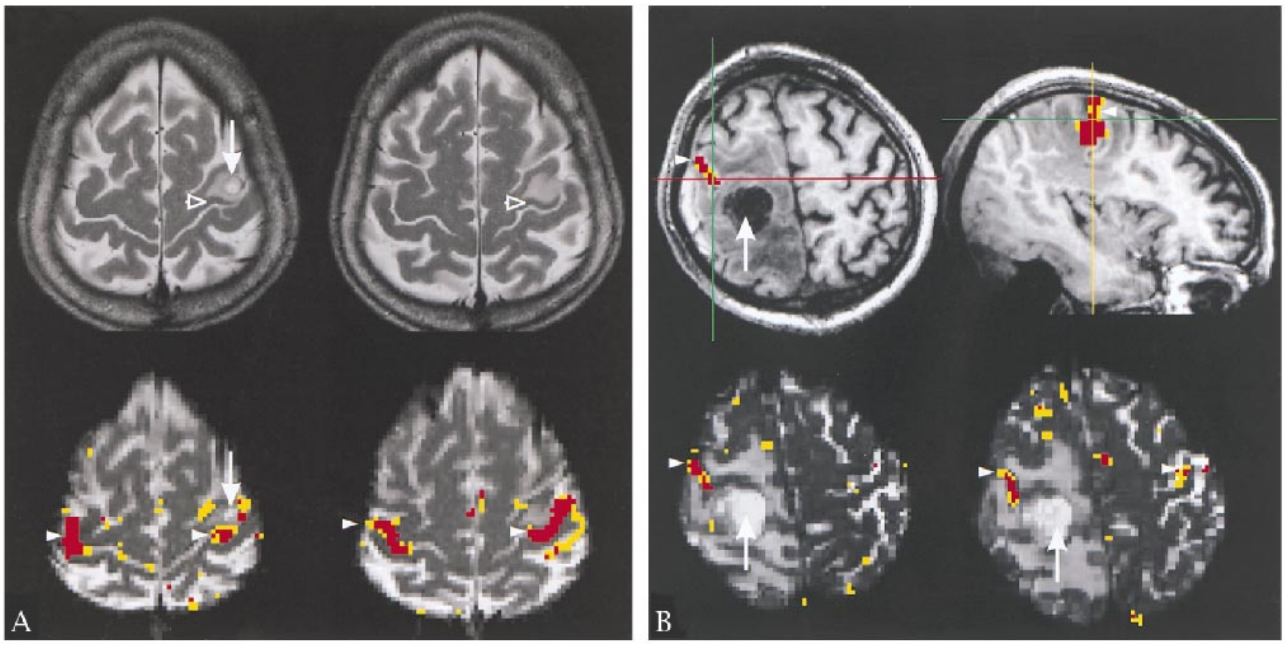

FIG 1. Adjacent to nonglial tumors, a normal volume of BOLD contrast enhancement was elicited.

A, Case 4. *Arrows* point to a small chronic abscess in the left precentral gyrus within the hand area. *Upper row* (T2-weighted turbo spin-echo sequence: 4500/120/1) shows edema apparently confined to the white matter. A narrow band of cortex is spared (*open arrowheads*). *Lower row* (echo-planar image: 3500/84/1), shows BOLD contrast enhancement in the cortex directly adjacent to the edema (*arrowheads*). Neither the edema nor the lesion affect the BOLD contrast enhancement.

B, Case 10. *Arrows* point to a metastatic lesion located in the right postcentral gyrus, slightly superior to the hand area. *Arrowheads* point to the functional activation of the sensorimotor cortex. *Upper row* is an overlay of the activation map onto the full head volume (MPRAGE: 9, 7/4/1 [TR/TE/excitations]). *Lower row* is an overlay onto the functional echo-planar sections (3500/84/1). In the ipsilateral hemisphere, the activation is squeezed between the swollen pre- and postcentral gyrus, but is not reduced. There is very little activation in the contralateral hemisphere.

occupying lesion, distance to the hand-motor area, and displacement of the hand-motor area) did not significantly correlate with the HAI ($P > .20$ in all cases). The type of tumor explained 24% of the variability of the HAI (R^2, Yates adjusted). After linear regression using type of tumor, the scatterplot of residuals showed random scattering. The analysis of variance detected a significant ($P > .05$) effect on the HAI, again for the type of tumor. The other parameters (paresis of the hand contralateral to the tumor and tumor on the dominant versus nondominant hemisphere) did not have any impact on the HAI.

Discussion

We have shown that different space-occupying lesions may have different effects on BOLD contrast enhancement. Near gliomas, BOLD contrast enhancement is significantly reduced in the pre- and postcentral gyrus, whereas it remains unaffected near nonglial space-occupying lesions. This concurs with the finding of BOLD contrast enhancement reduction in a case of grade IV glioma reported by Holodny et al (36). The authors suggested that the venous vessels were compressed because of the increased pressure in the area adjacent to the gliomas. The resulting reduction of the cortical blood volume would lead to a diminished BOLD contrast enhancement. Following this line of argument, the loss of BOLD contrast enhancement should be more pronounced the larger a tumor is and the greater its mass effect. Our data do not support this hypothesis in that tumor volume, proximity to the hand-motor area, and mass effect did not correlate with the HAI. Our data rather suggest that tumors exert little mechanical influence on BOLD contrast enhancement. Task-related changes in BOLD contrast enhancement occur in the cortical capillary bed and draining pial venules. As such, purely mechanical deformation of white matter tracts and their vasculature will not be expected to affect BOLD contrast enhancement among patients with deep intraaxial tumors.

We hypothesize that the invasive nature of gliomas and their capacity to elaborate neurotransmitters may account for the reduction in BOLD contrast enhancement seen in functional brain tissue adjacent to these lesions. This idea is corroborated by the absence of BOLD contrast enhancement in invaded cortex in the cases of patients 14 and 20 in our sample and in one case reported by Mueller et al (5). On the other hand, Nitschke et al (37) reported one case of glioma showing BOLD contrast enhancement within the perifocal edema. Until now, few comparable cases have been reported, because in most cases, cortical invasion was accompanied by major neurologic deficits. The absence of BOLD contrast enhancement within tu-

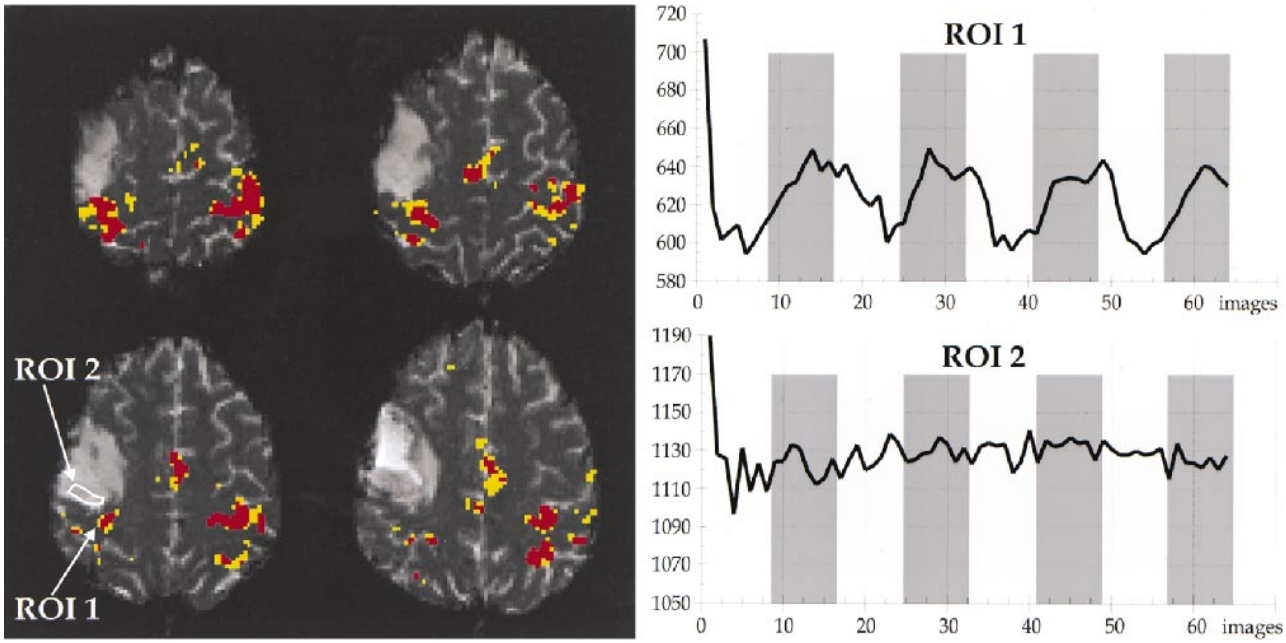

FIG 2. Case 20. The patient was suffering from an anaplastic astrocytoma invading the precentral gyrus. She presented with focal epileptic seizures of the face on the left side but did not have a motor deficit. Overlay of the activation map onto the functional echo-planar image (3500/84/1) shows activation nearly symmetrical in the upper two sections lining the Ω-shaped hand-motor area. There is less activation in the ipsilateral sensorimotor cortex on the lower two sections. The signal hyperintense parts of the sensorimotor cortex do not display BOLD contrast enhancement. Region of interest 1 is the cluster of activated voxels in the most medial part of the pre- and postcentral gyrus. Region of interest 2 is on the lateral continuation of the pre- and postcentral gyrus within an area of T2 signal hyperintensity of the cerebral cortex. The signal hyperintensity likely indicates gliomatous infiltration; in this case, histologic analysis of the resected specimen showed diffuse infiltration of the cortex. The interval of the signal intensity of region of interest 1 shows task-related signal changes (BOLD contrast enhancement) of approximately 6%, with hemodynamic delays of one to three images (*gray bars* indicate stimulation measurements). Region of interest 2 does not show BOLD contrast enhancement, although the analogous area in the left hemisphere is strongly activated.

mors is frequently reported (37, 38), except for cases of arteriovenous malformations, which have been reported by Maldjian (39) to show BOLD contrast enhancement in some cases. Nevertheless, cortical function may be preserved within tumors, as can be inferred from the intact motor function and has been proved by intraoperative cortical stimulation (40, 41). In case 20, no pareses, and in case 14, only mild pareses of the hand were found, indicating a mostly intact function of the sensorimotor cortex. Thus, we favor the hypothesis of a direct influence of the gliomas on the BOLD contrast enhancement over a secondary reduction of BOLD contrast enhancement attributable to reduced neuronal activity.

A hypothesis for the findings in case 6 (Fig 3) of reduced BOLD contrast enhancement in the ipsilateral hemisphere (HAI, 0.24) is the possibility of the secondary brain metastasis having neuroendocrine function similar to that found with the primary lesion in the lung. This exemplifies the idea that tumors synthesizing neurotransmitters have greater impact on BOLD contrast enhancement.

In the glioma group, BOLD contrast enhancement is reduced on the ipsilateral hemisphere, even if the two cases (cases 14 and 20) with macroscopic signs of invasion of the cortex were excluded from analysis. There probably is more than one mechanism to account for the reduction of BOLD contrast enhancement in tissue surrounding gliomas. A ''lo-

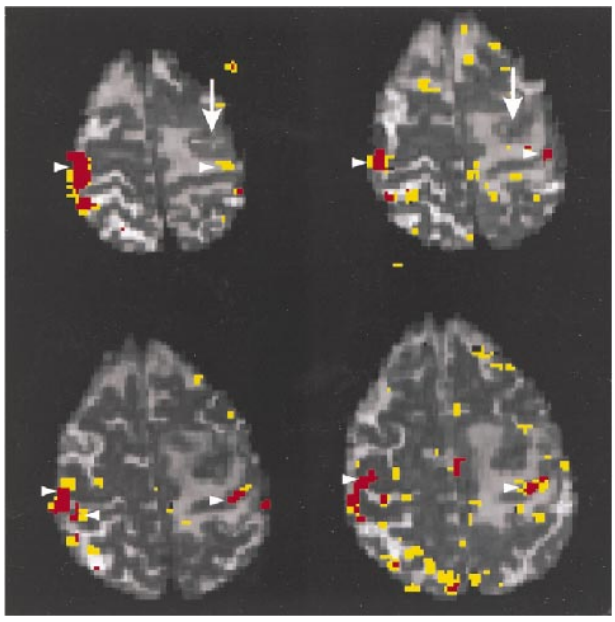

FIG 3. Case 6. *Arrows* point to a metastasis of a neuroendocrine active lung cancer located in the left precentral gyrus near the hand area. A large edema extends into the pre- and postcentral gyrus. The patient presented with focal epileptic seizures starting at the right hand, generalizing secondarily. *Arrowheads* point to clusters of activation in the sensorimotor cortex overlaid onto the functional echo-planar sections (3500/84/1). On the ipsilateral hemisphere, the functional activation is far less than on the contralateral hemisphere. The parieto-occipital clusters on the lowest section are attributable to head motion.

cal'' mechanism involving the destruction of intercellular contacts and signaling pathways could result from cortical invasion. Other mechanisms involving effects over a distance could result from derangement in metabolism and neurotransmitter distribution in and adjacent to gliomas (''long distance'' mechanisms).

Holodny et al (36) proposed that the reduction of BOLD contrast enhancement near a glioma could be attributed to a loss of autoregulation of the tumor vasculature. This probably accounts for the area directly adjacent to gliomas, where tumor vasculature is present. Because we found BOLD contrast enhancement reduction some distance from gliomas, we think that the proposed long-distance mechanisms work on the normal cortical vasculature. The release of nitric oxide by reactive astrocytes and macrophages at the brain-glioma interface (23) results in luxury perfusion and a reduced oxygen extraction fraction. Because deoxyhemoglobin levels are low to begin with, a reduced BOLD contrast enhancement can be expected.

Yoshiura et al (42) examined seven patients with brain tumors with and without paresis of the hand (three and four patients, respectively), using a motor task with the hand contralateral to the tumor. The ratio of the activated area in the sensorimotor cortex ipsilateral/contralateral to the hand motion was abnormally high in the patients with paresis. The authors suggested that the relative excess activation of the unaffected motor area reflects compensatory reorganization induced by the functional damage (42). In our sample, only four patients, two of whom had gliomas, had paresis of the hand. In comparison with the 11 patients without paresis, we found only a very small and insignificant difference in the HAI between the groups (patients with paresis, 0.88; others, 0.92). Thus, there is no evidence for (mild) paresis to account for the decreased BOLD contrast enhancement on the ipsilateral hemisphere. In addition, our data do not support the notion that compensatory reorganization causes excess activation on the contralateral hemisphere because the mean volumes of activation on the contralateral hemisphere were 122 voxels among patients with paresis and 170 voxels among the others.

The type of tumor explains 24% of the variability of the HAI (far more than any of the other parameters). Although this does not seem to be an impressive figure, it should be noted that even within a healthy participant, the variability of the HAI is high. We examined two participants with the same paradigm used for patients, 11 and 12 times, respectively, on different days. We found mean HAI of 1.26 $\pm$ 0.29 SD (23%) and 0.93 $\pm$ 0.19 SD (20%) for these participants (unpublished data). The variability between participants can be expected to be even larger. As such, the interindividual variability in activation may account for most of the variability in HAI in the patients with tumors that was not attributable to the type of tumor. The random scatter in the residual plot also supports this.

Hemispheric asymmetry in BOLD contrast enhancement has been reported to accompany hemispheric dominance (43). As the tumors grow on either hemisphere, the HAI will be computed, sometimes with the volume of activation on the dominant hemisphere in the numerator and sometimes in the denominator, further giving rise to variability of the HAI. This effect, however, was not significant in the present study.

Another source of variability may be a difference in motor performance between the two hands. We monitored the frequency and the extent of the movement but did not control for the force. In addition, it may pose a larger computational load to the ipsilateral hemisphere to perform the paradigm because of a partial impairment of the cortex, even if the motor output is symmetrical. This may affect the HAI in individual patients regardless of whether they suffer from a glioma or a nonglial lesion. Because we compared two groups of patients with tumors, we do not think there is a net effect on the mean HAI of the groups, but it will add to the variability of the index.

Conclusion

Near gliomas, BOLD contrast enhancement is significantly reduced, whereas it remains unaffected near nonglial space-occupying lesions. We propose two mechanisms to reduce BOLD contrast enhancement near gliomas. A local mechanism seems to be linked to cortical invasion. It seems not to result from reduced neuronal activity but works directly on the neurovascular coupling. It is interesting to note that during cortical invasion, the neurovascular coupling, at least in some cases, seems to break down before the cortical function is severely affected. A second long-distance mechanism is probably attributable to derangement in metabolism and neurotransmitter distribution.

Great care should be taken in the assessment of fMR mapping of eloquent areas in tumor patients because BOLD contrast enhancement, at least near gliomas, may be reduced or missing on functionally intact cortex. In a bad-case scenario, for example, a cluster of activated voxels would be rostral to a glioma, resulting from a motor task. That could mean that one is looking at the activated primary motor cortex and the glioma is located in the parietal brain. It, however, could also be the activated prefrontal cortex one is looking at, and the glioma is located in the precentral gyrus directly adjacent to the primary motor cortex. The functionally intact primary motor cortex does not show BOLD contrast enhancement because of the close proximity of the glioma.

Although the data are preliminary in this respect, it will be interesting to explore the possibility further to make use of the differential impact of gli-

omas and nonglial lesions on BOLD contrast enhancement in differentiating the type of tumor.

Usually, fMR imaging in patients is used to make inferences from the results of the functional imaging on the disease. We propose to use fMR imaging for patients to make inferences on the physiologic mechanisms of BOLD contrast enhancement in humans, taking into account the pathologic conditions the disease causes in the brain. This is especially valuable if it is possible to obtain a biopsy specimen of the brain for histologic and histochemical examination, such as from patients with brain tumors, and will also be interesting in cases of metabolic diseases.

Bimanual motor activation paradigms are helpful in the clinical setting because they provide BOLD contrast enhancement on the contralateral hemisphere as well. They can be used as an internal control of the quality of the fMR imaging examination and provide localization of the contralateral hand-motor area. This is useful because it allows the quantification of the mass effect of the tumor regarding the hand-motor area if the ipsilateral hand-motor area shows BOLD contrast enhancement as well. If the ipsilateral hand-motor area does not show BOLD contrast enhancement, the localization of the contralateral hand-motor area at least allows an educated guess regarding the localization of the ipsilateral hand-motor area.

Acknowledgments

The authors acknowledge the helpful comments and editorial advice provided by Michael Chee, MD.

References

1. Roux FE, Boulanouar K, Ranjeva JP, et al. **Cortical intraoperative stimulation in brain tumors as a tool to evaluate spatial data from motor functional MRI.** *Invest Radiol* 1999;34: 225–229
2. Pujol J, Conesa G, Deus J, Lopez-Obarrio L, Isamat F, Capdevila A. **Clinical application of functional magnetic resonance imaging in presurgical identification of the central sulcus.** *J Neurosurg* 1998;88:863–869
3. Schulder M, Maldjian JA, Liu WC, et al. **Functional image-guided surgery of intracranial tumors located in or near the sensorimotor cortex.** *J Neurosurg* 1998;89:412–418
4. Dymarkowski S, Sunaert S, Van Oostende S, et al. **Functional MRI of the brain: localisation of eloquent cortex in focal brain lesion therapy.** *Eur Radiol* 1998;8:1573–1580
5. Mueller WM, Yetkin FZ, Hammeke TA, et al. **Functional magnetic resonance imaging mapping of the motor cortex in patients with cerebral tumors.** *Neurosurgery* 1996;39:515–520
6. van Zijl PC, Eleff SM, Ulatowski JA, et al. **Quantitative assessment of blood flow, blood volume and blood oxygenation effects in functional magnetic resonance imaging.** *Nat Med* 1998; 4:159–167
7. Boxerman JL, Bandettini PA, Kwong KK, et al. **The intravascular contribution to fMRI signal change: Monte Carlo modeling and diffusion-weighted studies in vivo.** *Magn Reson Med* 1995;34:4–10
8. Kennan RP, Gao JH, Zhong J, Gore JC. **A general model of microcirculatory blood flow effects in gradient sensitized MRI.** *Med Phys* 1994;21:539–545
9. Ogawa S, Menon RS, Tank DW, et al. **Functional brain mapping by blood oxygenation level-dependent contrast magnetic resonance imaging: a comparison of signal characteristics with a biophysical model.** *Biophys J* 1993;64:803–812
10. Magistretti PJ, Pellerin L. **Cellular mechanisms of brain energy metabolism: relevance to functional brain imaging and to neurodegenerative disorders.** *Ann N Y Acad Sci* 1996;777:380–387
11. Dirnagl U, Niwa K, Lindauer U, Villringer A. **Coupling of cerebral blood flow to neuronal activation: role of adenosine and nitric oxide.** *Am J Physiol* 1994;267:H296–H301
12. Berger PC, Scheithauer BW. ***Tumors of the Central Nervous System.*** Washington, Armed Forces Institute of Pathology,1994;
13. Tyler JL, Diksic M, Villemure JG, et al. **Metabolic and hemodynamic evaluation of gliomas using positron emission tomography.** *J Nucl Med* 1987;28:1123–1133
14. Liwnicz BH, Wu SZ, Tew JM Jr. **The relationship between the capillary structure and hemorrhage in gliomas.** *J Neurosurg* 1987;66:536–541
15. Ji Y, Powers SK, Brown JT, Miner R. **Characterization of the tumor invasion area in the rat intracerebral glioma.** *J Neurooncol* 1996;30:189–197
16. Kuroiwa T, Nagaoka T, Ueki M, et al. **Correlations between the apparent diffusion coefficient, water content, and ultrastructure after induction of vasogenic brain edema in cats.** *J Neurosurg* 1999;90:499–503
17. Beaney RP, Brooks DJ, Leenders KL, Thomas DG, Jones T, Halnan KE. **Blood flow and oxygen utilisation in the contralateral cerebral cortex of patients with untreated intracranial tumours as studied by positron emission tomography, with observations on the effect of decompressive surgery.** *J Neurol Neurosurg Psychiatry* 1985;48:310–319
18. Rhodes CG, Wise RJ, Gibbs JM, et al. **In vivo disturbance of the oxidative metabolism of glucose in human cerebral gliomas.** *Ann Neurol* 1983;14:614–626
19. Ito M, Lammertsma AA, Wise RJ, et al. **Measurement of regional cerebral blood flow and oxygen utilisation in patients with cerebral tumours using 15O and positron emission tomography: analytical techniques and preliminary results.** *Neuroradiology* 1982;23:63–74
20. Nagano N, Sasaki H, Aoyagi M, Hirakawa K. **Invasion of experimental rat brain tumor: early morphological changes following microinjection of C6 glioma cells.** *Acta Neuropathol (Berl)* 1993;86:117–125
21. Hossmann KA, Linn F, Okada Y. **Bioluminescence and fluoroscopic imaging of tissue pH and metabolites in experimental brain tumors of cat.** *NMR Biomed* 1992;5:259–264
22. Linn F, Seo K, Hossmann KA. **Experimental transplantation gliomas in the adult cat brain: 3: regional biochemistry.** *Acta Neurochir (Wien)* 1989;99:85–93
23. Whittle IR, Collins F, Kelly PA, Ritchie I, Ironside JW. **Nitric oxide synthase is expressed in experimental malignant glioma and influences tumour blood flow.** *Acta Neurochir (Wien)* 1996; 138:870–875
24. Russell DS, Rubinstein LJ. ***Pathology of Tumours of the Nervous System.*** 5th ed. London: Hodder and Stoughton Limited;1989;
25. Araque A, Parpura V, Sanzgiri RP, Haydon PG. **Tripartite synapses: glia, the unacknowledged partner.** *Trends Neurosci* 1999;22:208–215
26. Oldfield RC. **The assesment and analysis of handedness: the Edinbourgh inventory.** *Neuropsychologia* 1997;9:97–113
27. Otte M, Schreiber A, Büchert M, Greenlee MW. **Spatial registration of functional and morphological MR images** [abstract]. *Neuroimage* 1997;5:417 Presented at 3rd International Conference of Functional Mapping of the Human Brain, Copenhagen, 1997.
28. Yousry TA, Schmid UD, Alkadhi H, et al. **Localization of the motor hand area to a knob on the precentral gyrus: a new landmark.** *Brain* 1997;120:141–157
29. Rumeau C, Tzourio N, Murayama N, et al. **Location of hand function in the sensorimotor cortex: MR and functional correlation.** *AJNR Am J Neuroradiol* 1994;15:567–572
30. White LE, Andrews TJ, Hulette C, et al. **Structure of the human sensorimotor system: II: lateral symmetry.** *Cereb Cortex* 1997; 7:31–47
31. Amunts K, Schlaug G, Schleicher A, et al. **Asymmetry in the human motor cortex and handedness.** *Neuroimage* 1996;4:216–222
32. Rombouts SA, Barkhof F, Hoogenraad FG, Sprenger M, Valk J, Scheltens P. **Test-retest analysis with functional MR of the activated area in the human visual cortex.** *AJNR Am J Neuroradiol* 1997;18:1317–1322
33. Ramsey NF, Tallent K, Van Gelderen P, Frank JA, Moonen CT, Weinberger DR. **Reproducibility of human 3D fMRI brain maps acquired during a motor task.** *Human Brain Mapping* 1996;4:113–121

34. Watanabe M, Tanaka R, Takeda N. **Magnetic resonance imaging and histopathology of cerebral gliomas.** *Neuroradiology* 1992; 34:463–469
35. Kelly PJ, Daumas-Duport C, Kispert DB, Kall BA, Scheithauer BW, Illig JJ. **Imaging-based stereotaxic serial biopsies in untreated intracranial glial neoplasms.** *J Neurosurg* 1987;66:865–874
36. Holodny AI, Schulder M, Liu WC, Maldjian JA, Kalnin AJ. **Decreased BOLD functional MR activation of the motor and sensory cortices adjacent to a glioblastoma multiforme: implications for image-guided neurosurgery.** *AJNR Am J Neuroradiol* 1999;20:609–612
37. Nitschke MF, Melchert UH, Hahn C, et al. **Preoperative functional magnetic resonance imaging (fMRI) of the motor system in patients with tumours in the parietal lobe.** *Acta Neurochir (Wien)* 1998;140:1223–1229
38. Roux FE, Boulanouar K, Ranjeva JP, et al. **Usefulness of motor functional MRI correlated to cortical mapping in rolandic low-grade astrocytomas.** *Acta Neurochir (Wien)* 1999;141:71–79
39. Maldjian J, Atlas SW, Howard RS II, et al. **Functional magnetic resonance imaging of regional brain activity in patients with intracerebral arteriovenous malformations before surgical or endovascular therapy.** *J Neurosurg* 1996;84: 477–483
40. Skirboll SS, Ojemann GA, Berger MS, Lettich E, Winn HR. **Functional cortex and subcortical white matter located within gliomas.** *Neurosurgery* 1996;38:678–684
41. Ojemann JG, Miller JW, Silbergeld DL. **Preserved function in brain invaded by tumor.** *Neurosurgery* 1996;39:253–258
42. Yoshiura T, Hasuo K, Mihara F, Masuda K, Morioka T, Fukui M. **Increased activity of the ipsilateral motor cortex during a hand motor task in patients with brain tumor and paresis.** *AJNR Am J Neuroradiol* 1997;18:865–869
43. Kim SG, Ashe J, Hendrich K, et al. **Functional magnetic resonance imaging of motor cortex: hemispheric asymmetry and handedness.** *Science* 1993;261:615–617